

Supporting Information

Highly stable CoMo₂S₄/Ni₃S₂ heterojunction electrocatalyst for efficient hydrogen evolution

Minmin Wang^{a,b†}, Mengke Zhang^{a,b†}, Wenwu Song^a, Weiting Zhong^a, Xunyue Wang^a, Jin Wang^{a, b,}, Tongming Sun^{a b*}, and Yanfeng Tang^{a,b*}*

^a *School of Chemistry and Chemical Engineering, Nantong University, Nantong 226019, China*

^b *Nantong Key Laboratory of Intelligent and New Energy Materials*

**Corresponding authors' E-mail:*

Jin Wang: wangjin110@ntu.edu.cn;

Tongming Sun: stm7314@ntu.edu.cn;

Yanfeng Tang: tangyf@ntu.edu.cn.

† These authors contributed equally to this work.

Experimental section

Materials

All chemicals were used directly without further purification. Cobalt (II) nitrate hexahydrate (AR, 99%), potassium hydroxide (AR, 90%) and thioacetamide (TAA) were purchased from Aladdin (Shanghai, China), ammonium molybdate tetrahydrate was acquired from Shanghai Shenbo Chemical CO. Ultrapure water ($18.5 \text{ M}\Omega \text{ cm}^{-1}$) was used throughout the whole experiments.

Synthesis of $\text{CoMo}_2\text{S}_4/\text{Ni}_3\text{S}_2$ samples

Typically, nickel foams (NF, $2 \text{ cm} \times 3 \text{ cm}$) were degreased by sonication in 3 M HCl solution for 20 min to remove oxides from the surface and then rinsed with acetone, ethanol and isopropanol for 10 min subsequently. Finally, the samples were dried at 60°C ovens for 12 h. Firstly, cobalt hydroxide nanocrystals were electrodeposited on the surface of nickel foam as the precursor: the electrodeposition was carried out in a standard three-electrode electrochemical cell containing NF as the working electrode, a platinum foil as the counter electrode and a Ag/AgCl (3 M KCl) as the reference electrode. The electrolyte bath contained 0.15 M $\text{Co}(\text{NO}_3)_2 \cdot 6\text{H}_2\text{O}$. The constant potential electrodeposition was then carried out at -1.0 V (versus Ag/AgCl) at room temperature. The optimized deposition time of Co has been determined to be 100 s. After deposition, the NF was carefully withdrawn from the electrolyte, rinsed with water and ethanol, then sonicated briefly in ethanol and left dry in air. Then 0.18 g of ammonium molybdate tetrahydrate was dissolved into 50 mL solution containing 80 mM thioacetamide. Then a piece of above Ni foam was put into the solution and transferred into a Teflon-lined stainless steel autoclave. After heating at 180°C for 10 h the Ni foam was taken out and cleaned by sonication in deionized water for 2 min to remove any possible contamination on the surface, and dried at 60°C overnight.

Characterizations

The as-synthesized samples were examined by powder X-ray diffraction (PXRD, BRUKER AXS D8 Advance, radiation source $\text{Cu K}\alpha$) at a 2θ range of 5° to 90° with scan speed $5^\circ \cdot \text{min}^{-1}$. The morphology was observed on field emission scanning electron microscope (FESEM, ZEISS Gemini SEM 300) and transmission electron microscopy (TEM, JEOL JEM-2100). The construction and binding energies of the samples were studied by X-ray photoelectron spectroscopy (XPS).

Electrochemical measurements

All electrochemical tests used a traditional three-electrode system by electrochemical workstation (CHI 660E) at room temperature. Ag/AgCl (saturated KCl) was used as reference electrode, carbon rod as counter electrode and as-prepared $1 \text{ cm} \times 1 \text{ cm}$ NF-based electrodes as working electrode. Linear sweep voltammetry (LSV) curves towards HER was measured at a scan rate of 1 mV s^{-1} after 100 cyclic voltammetry (CV) scans as activation in 1 M KOH ($\text{pH} = 14.0$). All the initial data were corrected for 80% iR loss and the potentials were transferred to a reversible hydrogen electrode (RHE) according to the formula of $E_{\text{vs.RHE}} = E_{\text{vs.Ag/AgCl}} + 0.197 \text{ V} + 0.059 \times \text{pH}$. Electrochemical impedance spectroscopy (EIS) was operated on the same three electrodes and 1 M KOH electrolyte, and the frequency range was from 0.01 to 10^5 Hz , and the amplitude was 10 mV. The electrochemical surface area (ECSA) was calculated by CVs in different scan rates from 20 mV s^{-1} to 60 mV s^{-1} . Amperometry i - t curve was carried out in 1 M KOH to test the samples' stability. Mott-Schottky (M-S) curve used a three-electrode system with

an applied frequency of 1 kHz and a potential amplitude of 10 mV/s. The Poisson equation was used to analyse the Mott-Schottky curve is:¹

$$\frac{1}{C_{SC}^2} = \frac{2}{eN_D\epsilon_0\epsilon} \left(E - E_{FB} - \frac{KT}{e} \right)$$

Carrier concentration (N_D , cm^{-3}) can be calculated using the slope of the Mott-Schottky curve:²

$$N_D = \left(\frac{2}{e\epsilon_0\epsilon} \right) \left[\frac{d(1/C_{SC}^2)}{dE} \right]^{-1}$$

E_{FB} is the flat band potential, $e = 1.6 \times 10^{-19}$ C, $\epsilon_0 = 8.85 \times 10^{-14}$ F/cm, ϵ is the permittivity of NiO (30).

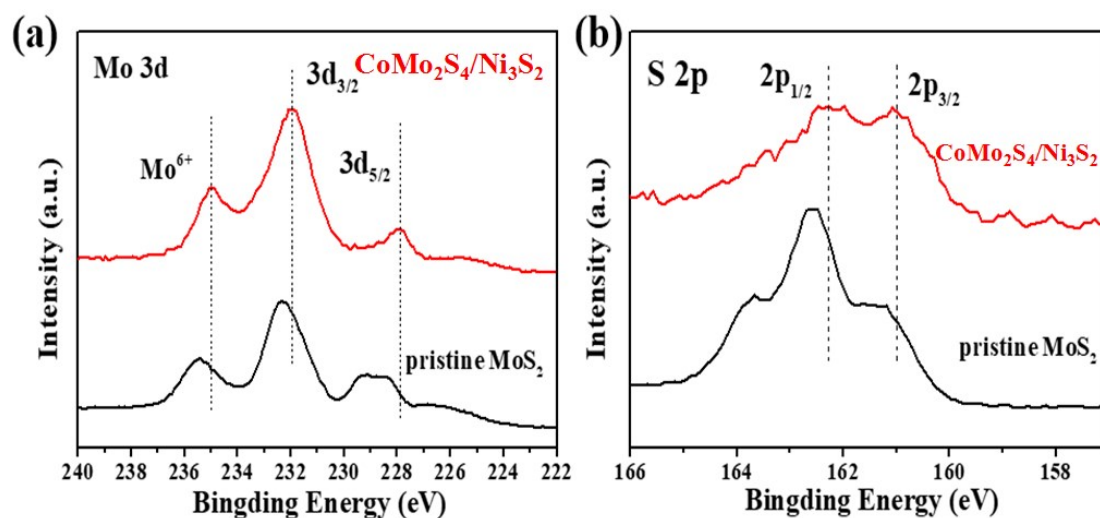


Fig. S1 XPS deconvoluted results comparison of (a) Mo 3d and (b) S 2p over pristine MoS_2 and $\text{CoMo}_2\text{S}_4/\text{Ni}_3\text{S}_2$.

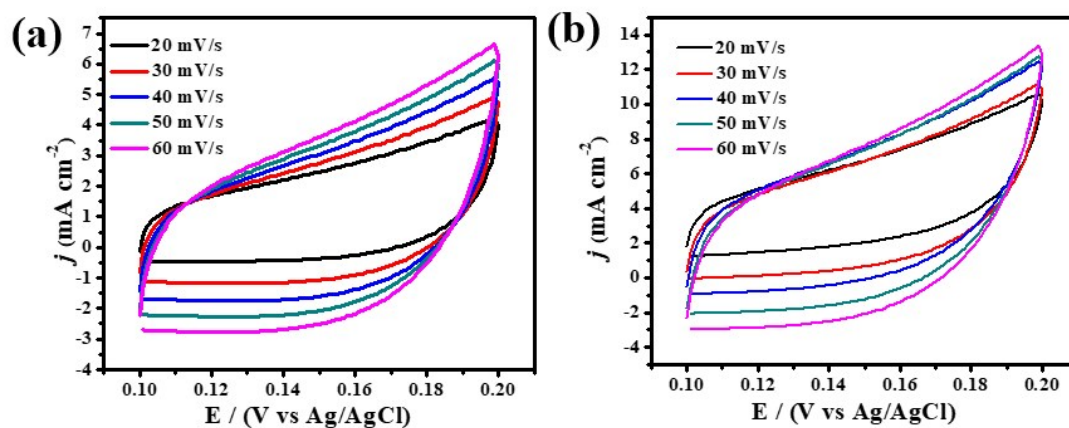


Fig. S2 Cyclic voltammograms at different scan rate in the region of 0.1-0.2 V vs. Ag/AgCl for (a) MoS_2 and (b) $\text{CoMo}_2\text{S}_4/\text{Ni}_3\text{S}_2$.

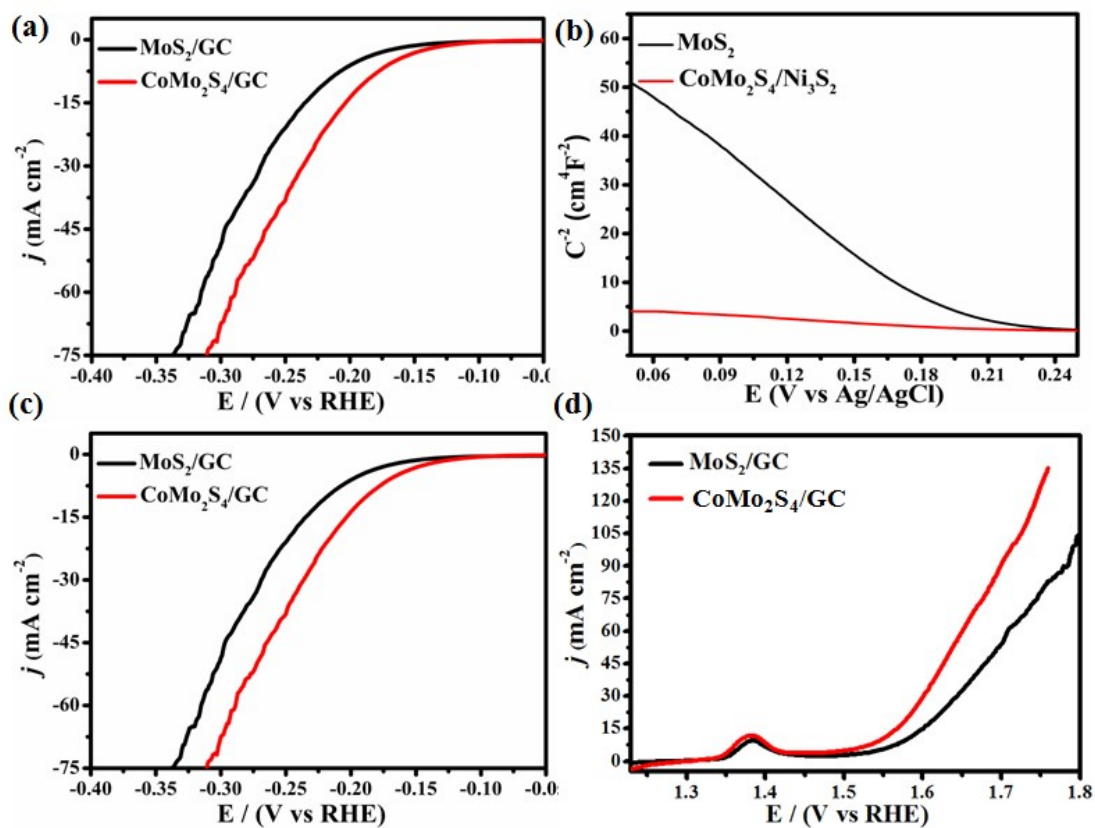


Fig. S3 (a) HER performance based on ECSA for MoS₂ and CoMo₂S₄/Ni₃S₂. (b) Mott-Schottky plots for MoS₂ and CoMo₂S₄/Ni₃S₂ at 1 kHz frequency in 1 M KOH (pH = 14) at room temperature. (c-d) HER and OER performance based on GC for MoS₂ and CoMo₂S₄ in 1 M KOH.

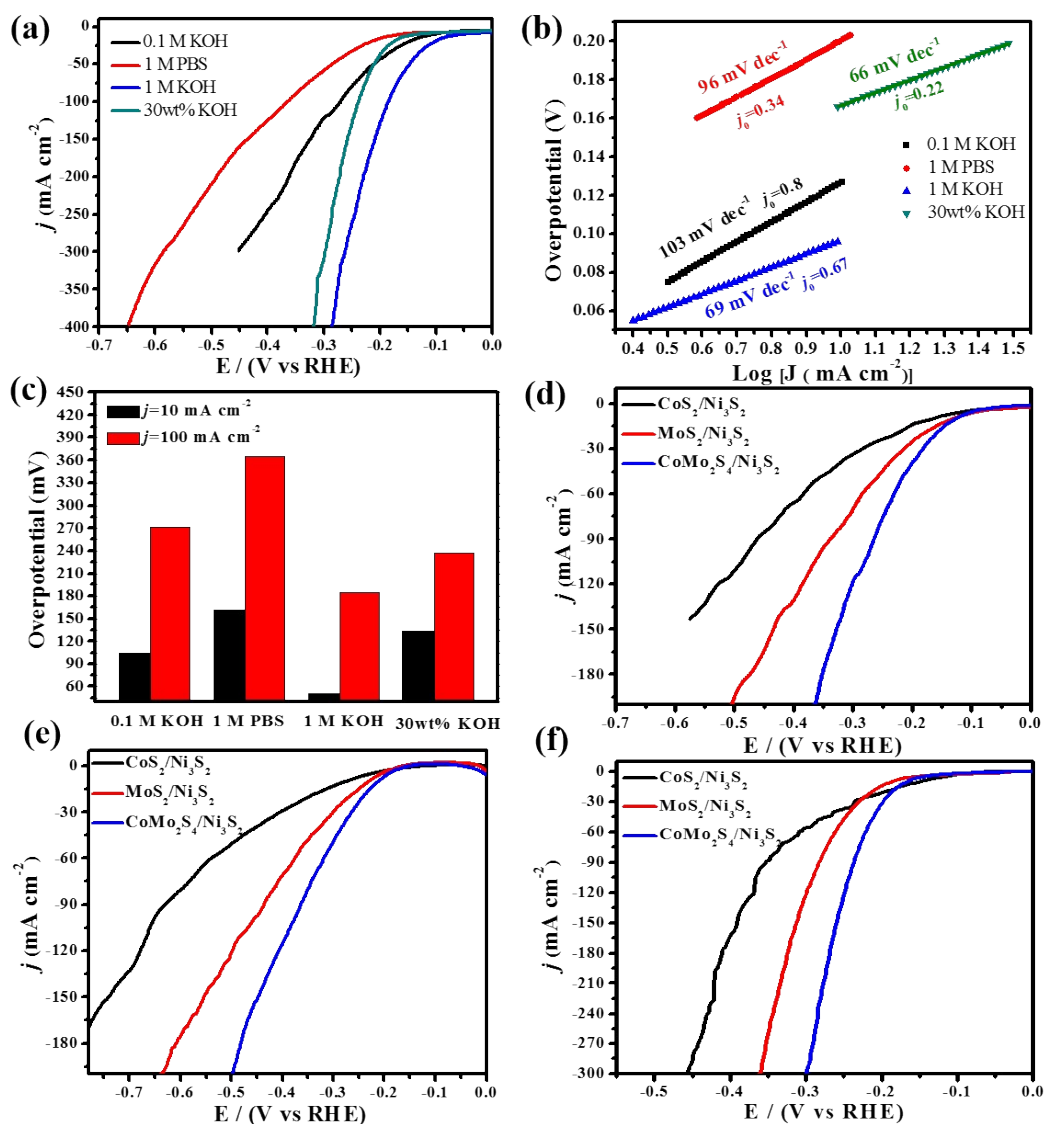


Fig. S4 (a) HER polarization curves of $\text{CoMo}_2\text{S}_4/\text{Ni}_3\text{S}_2$ in different electrolytes; (b) Tafel slopes and corresponding exchange current density (j_0); (c) Overpotentials at 10 and 100 mA cm⁻² for $\text{CoMo}_2\text{S}_4/\text{Ni}_3\text{S}_2$ electrode in different electrolytes. (d-f) HER polarization curves (1 mV s^{-1}) of different electrode in different electrolytes, (d) 0.1 M KOH; (e) 1 M PBS (pH=7); (f) 30wt% KOH solution.

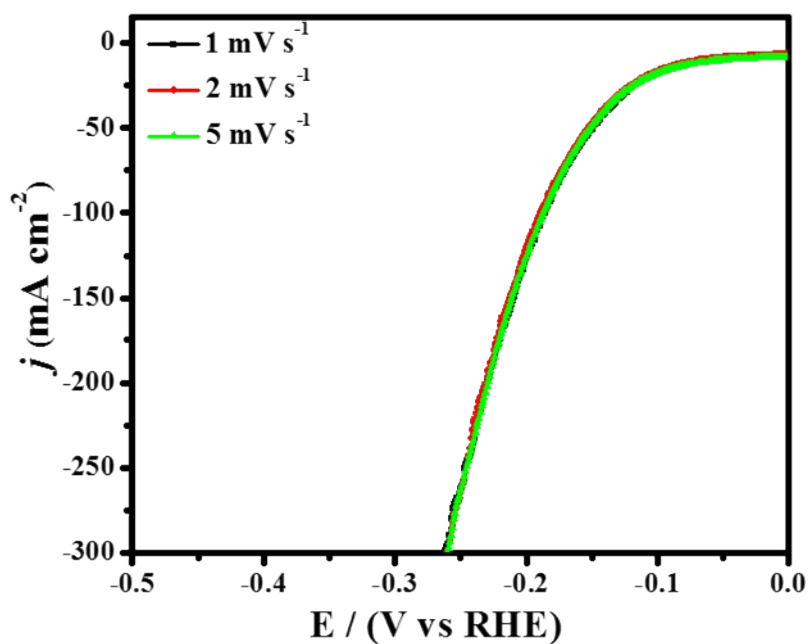


Fig. S5 HER polarization curves of CoMo₂S₄/Ni₃S₂ heterojunction under various sweep speeds.

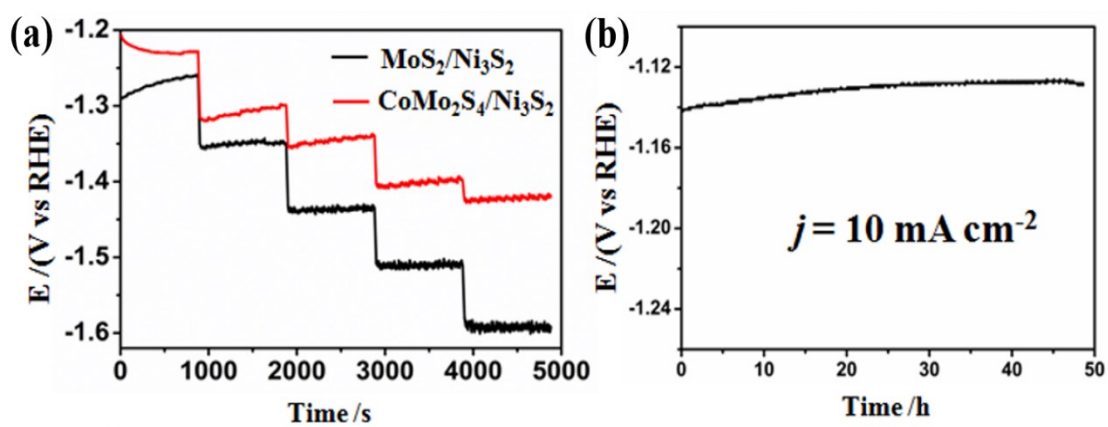


Fig. S6 (a) Multi-step current process obtained for the MoS₂/Ni₃S₂ and CoMo₂S₄/Ni₃S₂ electrodes. (b) Chronopotentiometric curve of HER for CoMo₂S₄/Ni₃S₂ at 10 mA cm⁻² in 1 M KOH.

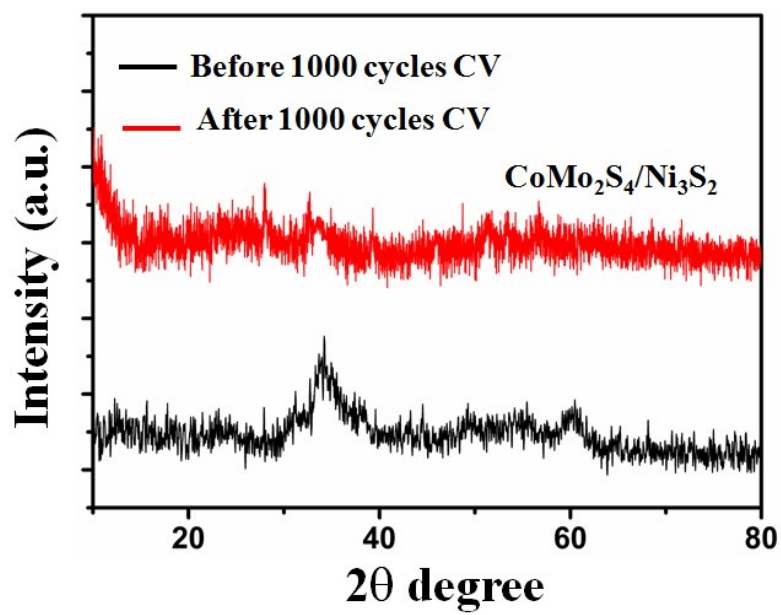


Fig. S7 PXRD patterns of $\text{CoMo}_2\text{S}_4/\text{Ni}_3\text{S}_2$ heterojunction before and after 1000 cycles CV.

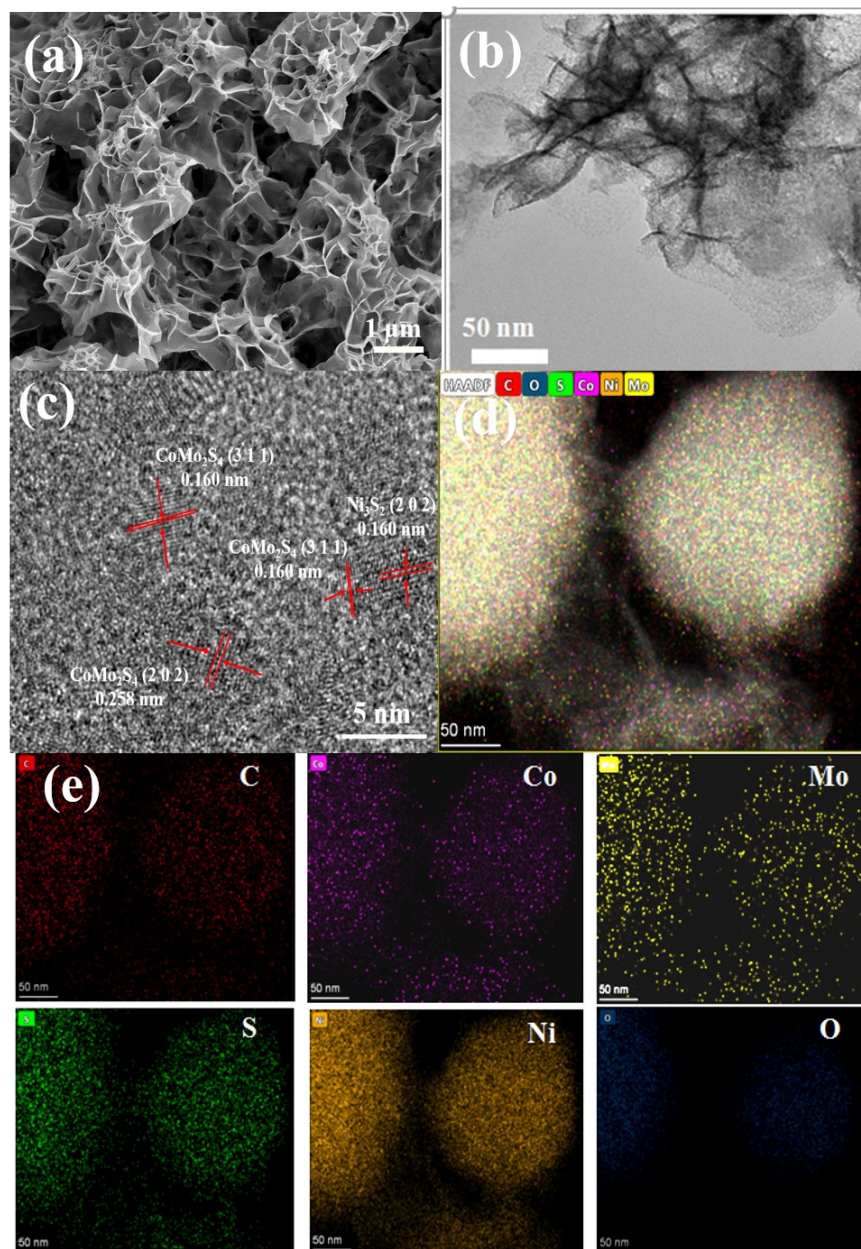


Fig. S8 (a) SEM, (b)TEM, (c) HRTEM images, and (d-e) its corresponding elemental mapping for the sample of $\text{CoMo}_2\text{S}_4/\text{Ni}_3\text{S}_2$ heterojunction after ~ 50 h chronopotentiometric test.

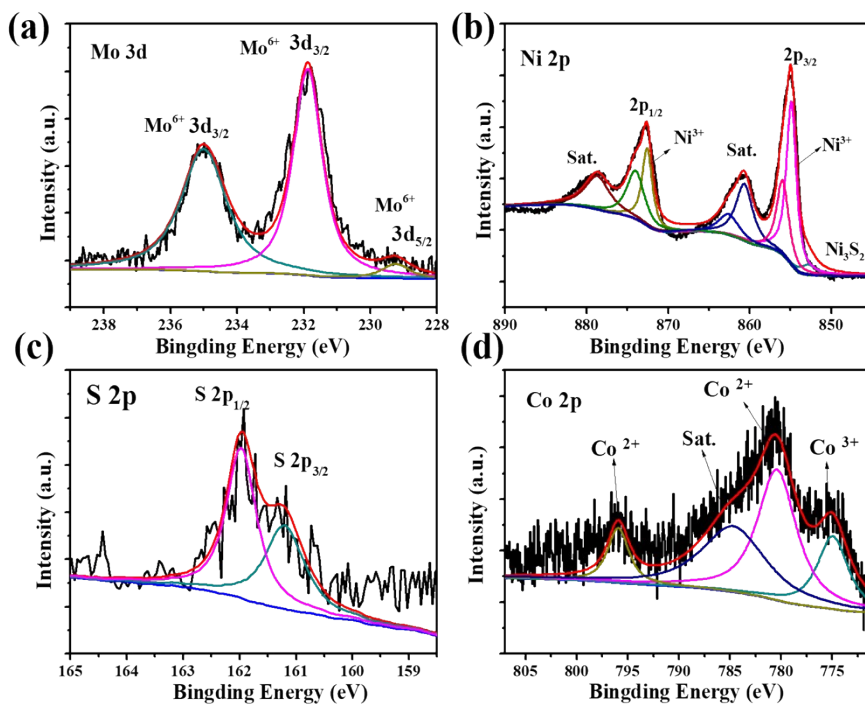


Fig. S9 XPS spectra of $\text{CoMo}_2\text{S}_4/\text{Ni}_3\text{S}_2$ heterojunction after ~ 50 h chronopotentiometric test.

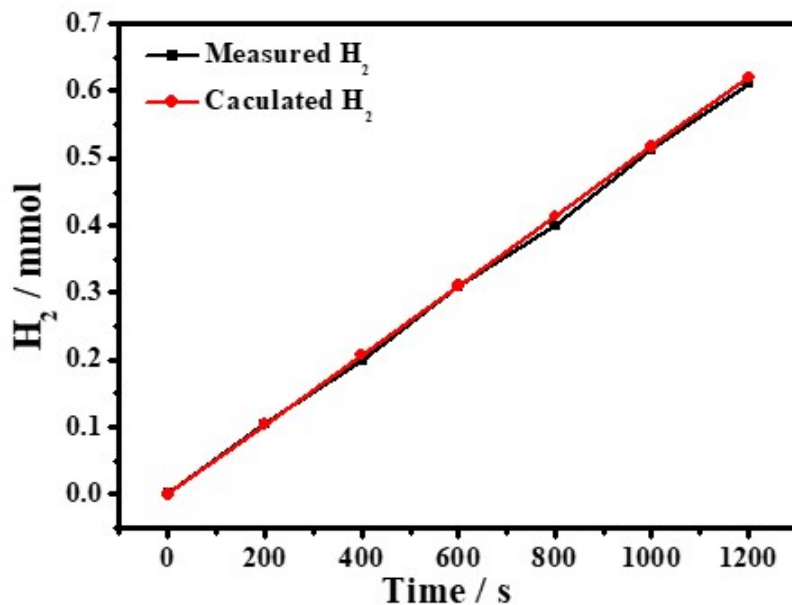


Fig. S10 The amount of gas theoretically calculated and experimentally measured versus time for HER at 100 mA cm^{-2} .

Reference

1. Chen, J. Z.; Li, B.; Zheng, J. F.; Jia, S. P.; Zhao, J. H.; Jing, H. W.; Zhu, Z. P., Role of One-Dimensional Ribbonlike Nanostructures in Dye-Sensitized TiO₂-Based Solar Cells. *J. Phys. Chem. C* **2011**, *115* (14), 7104-7113.
2. Wang, G. M.; Wang, H. Y.; Ling, Y. C.; Tang, Y. C.; Yang, X. Y.; Fitzmorris, R. C.; Wang, C. C.; Zhang, J. Z.; Li, Y., Hydrogen-Treated TiO₂ Nanowire Arrays for Photoelectrochemical Water Splitting. *Nano Lett.* **2011**, *11* (7), 3026-3033.